analytical chemistry

ARTICLE

pubs.acs.org/ac

Pellicular Particles with Spherical Carbon Cores and Porous Nanodiamond/Polymer Shells for Reversed-Phase HPLC

Landon A. Wiest,[†] David S. Jensen,[†] Chuan-Hsi Hung,[†] Rebecca E. Olsen,[†] Robert C. Davis,[‡] Michael A. Vail,[§] Andrew E. Dadson,[§] Pavel N. Nesterenko,[∥] and Matthew R. Linford*[,†]

[†]Department of Chemistry and Biochemistry and [‡]Department of Physics & Astronomy, Brigham Young University, Provo, Utah 84602, United States

[§]US Synthetic Corporation, Orem, Utah 84058, United States

[∥]Australian Centre for Research on Separation Science (ACROSS), School of Chemistry, University of Tasmania, Hobart 7001, Australia

Supporting Information

ABSTRACT: A new stationary phase for reversed-phase high performance liquid chromatography (RP HPLC) was created by coating spherical 3 μm carbon core particles in a layer-by-layer (LbL) fashion with poly(allylamine) (PAAm) and nanodiamond. Unfunctionalized core carbon particles were characterized by scanning electron microscopy (SEM), X-ray photoelectron spectroscopy (XPS), time-of-flight secondary ion mass spectrometry (ToF-SIMS), and Raman spectroscopy. After LbL of PAAm and nanodiamond, which yields ca. 4 μm core−shell particles, the particles were simultaneously functionalized and cross-linked using a mixture of 1,2-epoxyoctadecane and 1,2,7,8-diepoxyoctane to obtain a mechanically stable C_{18}/C_8 bonded outer layer. Core−shell particles were characterized by SEM, and their surface area, pore diameter, and volume were determined using the Brunauer−Emmett−Teller (BET) method. Short stainless steel columns (30 × 4.6 mm i.d.) were packed and the corresponding van Deemter plots obtained. The Supporting Information contains a MATLAB program used to fit the van Deemter data. The retentions of a suite of analytes were investigated on a conventional HPLC at various organic solvent compositions, pH values of mobile phases, including extreme pH values, and column temperatures. At 60 °C, a chromatogram of 2,6-diisopropylphenol showed 71 500 plates/m (N/m). Chromatograms obtained under acidic conditions (pH 2.7) of a mixture of acetaminophen, diazepam, and 2,6-diisopropylphenol and a mixture of phenol, 4-methylphenol, 2-chlorophenol, 4-chlorophenol, 4-bromophenol, and 1-*tert*-butyl-4-methylphenol are presented. Retention of amitriptyline, cholesterol, and diazinon at temperatures ranging from 35 to 80 °C and at pH 11.3 is reported. A series of five basic drugs was also separated at this pH. The stationary phase exhibits considerable hydrolytic stability at high pH (11.3) and even pH 13 over extended periods of time. An analysis run on a UHPLC with a "sandwich" injection appeared to reduce extra column band broadening and gave best efficiencies of 110 000−120 000 N/m.

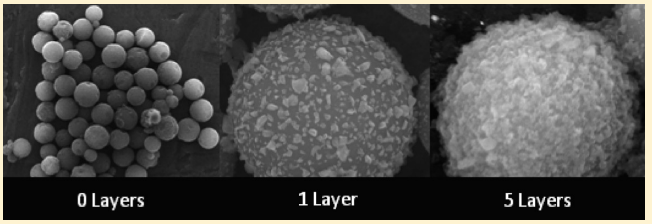

Silica is the workhorse of modern liquid chromatography.[1,2] Accordingly, its surface has been extensively studied and modified, which has led to a broad array of available functionalities for the chromatographer.[3] However, despite its flexibility, common silica-based stationary phases lack stability at both high and low pH, where the useful window of pH stability for a typical bonded phase lies between ca. 2 and 8.[4,5] A number of researchers have investigated ways to improve the stability of silica, especially for reversed-phase (RP) HPLC. For example, it has been known for decades that increasing the length of the *n*-alkyl chain in alkylsilica bonded phases or end-capping residual silanols with trimethylchlorosilane or hexamethyldisilazane can improve the hydrolytic stability of bonded phases.[6] A further improvement in the hydrolytic stability of alkylsilicas can be achieved using trichloroalkylsilanes instead of monochlorodimethylalkylsilanes.[4,7] Immobilization of trichloroalkylsilanes on silica in the presence of water causes polycondensation and formation of polymeric layers of good stability, although additional silanols are created during polymerization.[8] Kirkland et al. used sterically protected monofunctional silanes to increase the hydrolytic stability of alkyl-bonded phases in highly acidic mobile phases.[3,4] Sagliano and co-workers studied the effect of silane structure on resistance to acid hydrolysis and reported higher stabilities for silanes with bulky or long chain alkyl groups.[9]

Kirkland, Glajch, and Farlee disclosed the concept of bidentate silanes of the form $XR_2Si-B-SiR_2X$, where −X is a reactive group such as −Cl or −OMe and −B− is a bridging group of variable nature and length, e.g., it may be an ethylene ($-CH_2CH_2-$) moiety or an oxygen atom, and R is a methyl, *n*-butyl, *n*-octyl, or *n*-octadecyl group.[4,10] Their C_{18}/C_{18} bidentate silane with

Received: October 12, 2010
Accepted: May 31, 2011
Published: June 20, 2011

a propylene bridge as a bonded phase had a very low rate of hydrolysis in mobile phases at both low (0.9) and high (≥11) pH .[10,11]

Another possible improvement in the hydrolytic stability of silica particles is polymer shielding or cross-linking of bonded groups. Kobayashi and co-workers treated octyltrichlorosilane modified silica with a cyclic siloxane monomer, effectively end-capping the bonded phase with a siloxane polymer to improve its stability.[12] Carr and co-workers chemisorbed (chloromethyl)-phenylethyltrichlorosilane ($ClCH_2C_6H_4CH_2CH_2SiCl_3$) onto silica and then cross-linked it via Friedel−Crafts alkylation to itself and to a styrene heptamer or triphenylmethane.[13] When it was found that this phase was overly silanophilic compared to a steric-protected C_{18} phase, i.e., it had too many residual silanols that were leading to peak tailing of basic analytes, a monolayer of a monofunctional silane, $ClCH_2C_6H_4CH_2CH_2Si(CH_3)_2Cl$, was deposited, which was then similarly cross-linked with the styrene heptamer. While this assembly was not more stable than the layer prepared with the trifunctional silane ($ClCH_2C_6H_4CH_2CH_2SiCl_3$), it could be further cross-linked and then modified with C_8 groups, also via Friedel−Crafts alkylation, to produce an extremely stable phase. This material showed substantially lower silanophilicity than before; the peak shapes in the resulting separations of basic drugs were at least as good as those obtained using a steric-protected C_{18} phase.[14]

The work cited above focuses on improvements in the low pH stability of bonded phases on silica. An approach for the improvement of the hydrolytic stability of hydrophobic column packings at higher pH values is based on the synthesis of various inorganic−organic hybrid materials. For example, a group at Waters Corp. (Milford, MA) first formed particles by condensing methyltriethoxysilane, $CH_3Si(OCH_2CH_3)_3$, and tetraethoxysilane ($Si(OCH_2CH_3)_4$, TEOS), which placed methyl groups within and at the surfaces of the particles.[15] These first generation hybrid particles comprise the company's XTerra product line. They can be functionalized with C_8 and C_{18} silanes, and show reduced tailing of basic analytes, consistent with a reduction of silanol quantity and activity. A further advance from this group came by the use of silanes with bridging alkyl groups, e.g., $(CH_3O)_3SiCH_2CH_2Si(OCH_3)_3$, which is the basis of their bridged ethyl hybrid technology in their XBridge and ACQUITY product lines.[16,17] Columns packed with the resulting particles were stable for 140 h at 50 °C in a pH 10 triethylamine-containing mobile phase.[17]

A similar series of inorganic−organic hybrid stationary phases was produced by Phenomenex (Torrance, CA) under the trade name Gemini. Gemini particles consist of a traditional silica core surrounded by an inorganic−organic layer, similar to that of the Waters XTerra particles. Their TWIN-NX technology uses ethylene bridged silanes, like those in Waters' XBridge and ACQUITY products. The temperature and pH-stabilities of the Gemini C_{18}, Gemini C_{18} NX, and XBridge C_{18} columns were recently compared. The Gemini C_{18} column was substantially less stable than the Gemini C_{18} NX, which in turn was less stable than the XBridge C_{18}.[18] In general, the prolonged stability of inorganic−organic hybrid stationary phases in mobile phases at pH 10.0−10.5 has been demonstrated.

Clearly notable advances have been made with regards to creating stable, effective, silica-based materials. However, Teutenberg and co-workers recently compared the stabilities of a series of commercially available columns that are advertised as highly stable and concluded that: "Although some progress has been made to increase the stability of packing materials at very high and low pH, further improvements of silica-based stationary phases regarding dissolution at high temperatures still is a challenge."[18] It appears that a considerable need remains for future innovation.

A significant motivation for creating HPLC stationary phases/supports that are stable at high pH exists in the pharmaceutical industry. McCalley and co-workers[19,20] expressed the difficulty of separating basic compounds under reversed-phase conditions because these analytes usually exist in their protonated states under the pH conditions appropriate for most silica-based columns. (Protonated species are typically less retained under reversed-phase conditions than the corresponding unprotonated ones.[21]) Thus, high pH values (at least high enough to deprotonate amines) would be advantageous in such separations. McCalley further observes that of all pharmaceutical compounds, 70% are bases.[19] Because the pK_a values of most amines are ca. 9.5−11, and at least in aqueous solutions, the pH must be at least one pH unit above the pK_a value of an acidic moiety for ca. 90% or more of these groups to be deprotonated, there is a strong need for a chromatographic material that can withstand a pH where the basic groups on analytes would be largely or even entirely deprotonated. (Note that in this work when we mention the "pK_a of an amine," we are, technically speaking, referring to the pK_a of the conjugate acid of that amine.)

Because of the considerable need to create highly stable stationary phases, other, nonsiliceous materials have also been studied. Some of these supports, which include organic polymers, zirconia, titania, alumina, and porous graphitic carbon (PGC), are usually stable over a wide pH range but sometimes lack efficiency.[22−26] Carr and co-workers developed polymer coated or encapsulated zirconia as both hydrophilic (normal-phase HPLC) and hydrophobic (reversed-phase HPLC) stationary phases,[27−30] where these materials also have stability over a wide pH range.[24,31,32] However, due to Lewis acid sites on the zirconia surface, undesirable secondary interactions occur with certain analytes.[33−35] These specific interactions with analytes bearing carboxylic and phosphonic acid functional groups, in conjunction with the difficulty associated with functionalizing the zirconia surface,[30] help explain why zirconia-based supports/phases have not become more mainstream products.

PGC is an important material that has been marketed commercially since 1988 by more than one firm, e.g., Hypercarb by Thermo Scientific.[36,37] PGC is stable at extreme pH values and also elevated temperatures, although its selectivity is very different from standard reversed phases and noticeable tailing is observed with many analytes. While these differences/limitations have prevented it from being more widely adopted, there is currently a great deal of interest in this material because of its stability and unique selectivity to hydrophilic compounds.

Diamond has also been studied as a support/stationary phase in liquid chromatography.[38] For example, Nesterenko and co-workers employed sintered, microdispersed detonation nanodiamond for normal-phase separations[39] and ion exchange chromatography.[40] They performed baseline separations of various compounds using their normal-phase material and achieved 15 400 plates/m (N/m). Their peaks showed considerable asymmetry, especially at longer retention times. In more recent work they have achieved 45 300 N/m.[41]

Work in the Linford group at Brigham Young University has focused on the chemical modification of diamond and its subsequent use in solid-phase extraction (SPE) and HPLC. Their first separations were performed on poly(allylamine) (PAAm)-coated 50−70 μm diamond particles,[42,43] where SPE of lipids

was demonstrated. It was later shown that various alkyl and a perfluoroalkyl isocyanate would react with the PAAm-coated diamond, forming urea linkages between the isocyanate and PAAm.[44] SPE of pesticides from water was performed on the resulting C_{18} phase. Deuterium-terminated diamond (DTD),[45] was also shown to react with di-*tert*-amyl peroxide, and it could be further functionalized with polymers by radical polymerization.[46] The resulting diamond materials could be used for SPE. In general, these materials were stable under extreme pH conditions.[43,44]

In spite of these advances, the nonporous particles employed in these earlier studies would probably not be suitable for HPLC. Hence, pellicular particles[47] were formed by coating irregularly shaped ca. 1.7 μm diamond particles with bilayers of PAAm and nanodiamond in a layer-by-layer (LbL) fashion.[48] These PAAm-coated core−shell particles were then reacted with 1,2-epoxyoctadecane, creating a hydrophobic phase, where the C−N bond produced during the reaction between an amine and an epoxide is very resistant to hydrolysis at both low and high pH. This stationary phase was able to separate pesticides (cyanazine and diazinon) and various alkylbenzenes. An efficiency of 54 800 N/m was obtained with diazinon, which was a solid improvement over previous diamond-based materials. Unfortunately, after an extended period of time, the material began to degrade. Another PAAm/nanodiamond pellicular phase, this time cross-linked/functionalized with 1,2,5,6-diepoxycyclooctane, was then prepared, and this material showed considerably improved stability, albeit lower efficiencies. However, even with this improved stability, back pressures were high for all of the particles made with irregular diamond particles.

While this earlier work was a step forward, a variety of issues needed to be addressed. First, it would be important to find a spherical, inert support to serve as the core for these particles, where this material would need to be amenable to functionalization via LbL chemistry. A spherical core would also be important because irregular diamond particles would be expected to have a significant negative impact on the eddy diffusion and flow distribution component in peak broadening (the *A* term in the van Deemter equation) and give a higher backpressure. In addition, it was imperative to find a way to stabilize this hydrophobic phase with some sort of cross-linker so that these phases would be mechanically stable over a longer period of time, but without a loss of efficiency.

In this work, we address these and other issues, showing the development of a new type of stationary phase created by coating spherical, 3 μm carbon particles with layers of PAAm and nanodiamond. The two types of stationary phases described herein are both hydrophobic (C_{18}), but one phase was also cross-linked. As expected, the non-cross-linked phase shows low mechanical stability, but the cross-linked material showed good stability over an extended period of time, and at high pH. Particular improvements over our last study[48] include the following: (1) Spherical carbon particles are used as cores instead of irregular diamond particles. (2) Efficiencies for these new core−shell particles are higher than those for the previous particles, in spite of the fact that the new particles are larger. (3) Two epoxides (a monofunctional epoxide and a bifunctional epoxide) are used in the functionalization/cross-linking of the PAAm/nanodiamond layers, where the monofunctional epoxide provides C_{18} chains and the bifunctional epoxide provides cross-linking. (4) These new particles are demonstrated to be hydrolytically stable for prolonged periods of time in both alkaline mobile phases (at pH 11.3 and even pH 13) and in acidic mobile phases (at pH 2.7). (5) Reduced column back pressures, i.e., higher possible flow rates, allow, for the first time in our work on diamond-containing pellicular particles, acquisition of complete van Deemter curves in a suitable range of flow rates. An analysis of these curves is presented. (6) Pressure-flow curves are reproducible/repeatable. (7) By appropriate particle preparation, relatively tight particle size distributions can be obtained, which translates into the improved mass transfer and expected flattening of the van Deemter curves at increasing flow rates. (8) Many different analytes are separarted on a conventional HPLC, including the alkylbenzenes, a series of basic drugs, and various phenols, at either pH 2.7 or pH 11.3. Indeed, more than 70 000 N/m were obtained for 2, 6-diisopropylphenol at 60 °C under acidic conditions. (9) A "sandwich" injection on a UHPLC system yielded 110 000−120 000 N/m for three low molecular weight analytes.

Note: The Supporting Information of this paper contains a short MATLAB program that accepts and plots van Deemter data, the contributions of the *A*, *B*, and *C* terms to the van Deemter expression, and the residuals to the fit. It further provides values of the rmse and R^2 for the fit, and the optimal values of *u* and *H*.

EXPERIMENTAL SECTION

Reagents and Materials. Table 1 gives the chemicals and materials used to create and test the phases in this work.

Empty stainless steel HPLC columns (30 mm × 4.6 mm i.d. with 0.5 μm frits) were obtained from Restek, Bellefonte, PA, and 50 mL centrifuge tubes were from Sarstedt, Newton, NC. All analyte solutions were prepared by mixing ca. 20 μL of an analyte in 15 mL of acetonitrile.

Instrumentation. Our HPLC consisted of a dual wavelength detector (Model No. 2487), a binary HPLC pump (Model No. 1525), and a column oven (Model Number 5CH) all from Waters Corporation, Milford MA. The LC system was run using Breeze, Version 3.3 Software. To calculate efficiencies, the software measured the full width at half-maximum (fwhm) of a peak and employed the equation, $N = 5.54(R_t/W_{1/2})^2$. Separations performed at the University of Tasmania were done using a Waters Alliance HPLC. A dual wavelength detector (Model No. 2487) was used for detection and the pump, autosampler, and column oven were all part of a 2695 Separations Module. The system was run using Empower, Version 2 software and efficiencies were calculated using the fwhm method. Column Packer: Pack-in-a-Box, 10 000 psi pump (Chrom Tech, Inc., Apple Valley, MN). All separations were performed under isocratic conditions. For the high and low pH separations, the pH of the water was set to 11.3 by addition of 0.1% (v/v) triethylamine, 13.0 by addition of tetramethylammonium hydroxide, or 2.7 by addition of formic acid. Analytes were injected using a 20 μL sample loop. Scanning electron microscope: Philips XL30 ESEM FEG (FEI Corporation, Hillsboro, OR). Samples for SEM were prepared by placing a slurry of particles directly on a stub and then drying the samples in an oven. Imaging was done under high-vacuum conditions with a spot size of 3. (This is an arbitrary number commonly used in SEM that has no units. This number represents the size of the aperture that allows electrons through for imaging.) Surface area analyzer (Brunauer−Emmett−Teller (BET) isotherm measurements): Micromeritics TriStar II (Micromeritics Instrument Corporation, Norcross, GA). Specific surface areas of the samples were determined from N_2 adsorption at 77 K. The samples were degassed at 200 °C for 12 h prior to data collection. Particle size distribution analyzer: Beckman Coulter LS

Table 1. Chemicals and Materials Used

chemical name	CAS No.[a]	manufacturer	location	purity
acetaminophen	103−90-2	Sigma-Aldrich	St. Louis, MO	BioXtra, ≥ 99.0%
acetonitrile	75-05-8	EMD	Gibbstown, NJ	HPLC grade
amitriptyline hydrochloride	549-10-8	Restek	St. Louis, MO	≥98%
benzenoid hydrocarbon kit		Supelco	St. Louis, MO	varied by analyte
4-bromophenol	106-41-2	Sigma-Aldrich	St. Louis, MO	99%
2-*tert*-butyl-4-methylphenol	2409-55-4	Sigma-Aldrich	St. Louis, MO	99%
2-chlorophenol	95-57-8	Sigma-Aldrich	St. Louis, MO	98%
4-chlorophenol	106-48-9	Sigma-Aldrich	St. Louis, MO	≥99%
cholesterol	57-88-5	Sigma-Aldrich	St. Louis, MO	approx 95%
clomipramine	303-49-1	Sigma-Aldrich	St. Louis, MO	≥98%
cyclohexanol	109-93-0	Fisher Scientific	Fair Lawn, NJ	reagent grade
diazepam	439-14-5	Sigma-Aldrich	St. Louis, MO	98%
diazinon	333-41-5	Fluka	Steinheim, Germany	Pestanal, analytical standard
1,2,7,8-diepoxyoctane	2426-07-51	Sigma-Aldrich	St. Louis, MO	97%
2,6-diisopropylphenol	2078-54-8	SAFC Supply Solutions	St. Louis, MO	97+%
doxepin hydrochloride	1229-29-4	Sigma-Aldrich	St. Louis, MO	
1,2-epoxyoctadecane	7390-81-0	Alfa Aesar	Ward Hill, MA	technical grade, 90%
imipramine	50-49-7	Sigma-Aldrich	St. Louis, MO	BioXtra, ≥99.0%
isopropyl alcohol	67-63-0	Mallinckrodt Baker Inc.	Phillipsburg, NJ	ChromAR
methanol	67-56-1	Fisher Scientific	Fair Lawn, NJ	HPLC grade
4-methylphenol	106-44-5	Supelco	St. Louis, MO	analytical standard
nanodiamond		Advanced Abrasives Corp.	Pannsauken, NJ	8.32 wt %, 0−100 nm
phenol	108-95-2	Sigma-Aldrich	St. Louis, MO	∼99%
poly(allylamine), avg 17 000 M_w	30551-89-4	Sigma-Aldrich	St. Louis, MO	20 wt % in water
poly(allylamine), avg 65 000 M_w	30551-89-4	Sigma-Aldrich	St. Louis, MO	20 wt % in water
spherical glassy carbon, 3 μm mean size		Supelco	St. Louis, MO	prototype material, not commercially available
tetramethylammonium hydroxide	75-59-2	Sigma-Aldrich	St. Louis, MO	24 wt % solution in water
triethylamine	121-44-8	Mallinckrodt Baker Inc.	Phillipsburg, NJ	99.50%
Triton X-100	9002-93-1	Fisher Scientific	Fair Lawn, NJ	electrophoresis grade
water	7732-18-5	From a Millipore system	Billerica, MA	18 MΩ resistivity (Milli-q System)
xylenes	1330-20-7	Mallinckrodt Baker Inc.	Phillipsburg, NJ	ACS grade

[a] Supplied by author.

13 320 Multi-Wavelength Particle Size Analyzer (Beckman Coulter, Inc., Brea, CA). Particle size distributions were obtained by placing drops of a suspension of particles in an analysis bath. X-ray photoelectron spectroscopy (XPS) was performed with an SSX-100 instrument from Surface Sciences (maintained by Service Physics in Bend, OR) using an Al Kα source and a hemispherical analyzer. An electron flood gun was employed for charge compensation, and this charge compensation was further enhanced with a fine Ni mesh approximately 0.5−1.0 mm above the surface of the sample. Survey scans, as well as narrow scans, were recorded with an 800 μm × 800 μm spot. Carbon powders were mounted onto double-sided tape adhered to silicon wafers for XPS analysis. Static time-of-flight secondary ion mass spectrometry (ToF-SIMS) was performed on an ION TOF IV instrument (Münster, Germany) with a 25 keV Ga^+ source and a 200 μm × 200 μm sample area. For ToF-SIMS analysis, the carbon powders were mounted onto double-sided tape adhered to silicon wafers. Raman spectroscopy was performed on a Chromex Raman 2000 instrument (Billerica, MA) with a 532 nm laser, the CCD was cooled to −40 °C, and the slit width was set at 100 μm. Raman spectra were obtained using conventional methods; loose powder was placed in a sample vessel and analyzed.

Particle Preparation. Particles were prepared using a layer-by-layer (LbL) procedure that was similar to that performed by Saini et al. on diamond core particles.[48] About 0.5 g of spherical, carbon particles, 3 μm in diameter, were suspended in 40 mL of a 1:1 water:methanol (H_2O:MeOH) mixture containing 3.3 mL of a 65 000 M_w poly(allylamine) (PAAm) solution, as obtained from

dx.doi.org/10.1021/ac200436a |*Anal. Chem.* 2011, 83, 5488–5501

the vendor. The particles were stirred for 24 h in this solution. The particles were then placed in a 50 mL screw cap plastic centrifuge tube, centrifuged at 5000 rpm, and rinsed three times with the 1:1 H_2O:MeOH solution. Nanodiamond (1.5 mL of a 8.32 wt % slurry) was then added to the PAAm coated particles that were suspended in ca. 40 mL of the rinse solution. The solution with the partially coated particles and nanodiamond was shaken by hand for 5 min and allowed to settle for 1 min. It was then centrifuged and rinsed twice with the 1:1 H_2O:MeOH mixture to remove excess nanodiamond from the particles. To these particles, now coated with a layer of PAAm and nanodiamond, was added 1.5 mL of a 7.5 wt % aqueous solution of PAAm (17 000 M_w). The particles were again agitated by hand for 5 min and allowed to settle for 1 min. Excess PAAm was removed by centrifuging the particles and rinsing three times with the same H_2O:MeOH mixture. Deposition of nanodiamond (8.32 wt % slurry) and PAAm (17 000 M_w) was subsequently performed in alternating steps until the desired thickness of the porous shell was reached, terminating in a PAAm coating. To clarify, 60 discrete depositions were performed to form the polymer-nanodiamond shell; to create a particle with a 0.5 μm shell, 30 bilayers were deposited. Deposition occurred in a similar manner to that observed by Saini in his work.[48] There appeared to be an induction period in which the surface was only partially covered, after which deposition appeared to proceed with greater regularity. The thickness was measured periodically during particle growth by scanning electron microscopy.

Particle Optimization. In an effort to improve the particle size distribution, two other batches of particles were prepared. One batch of core particles was sonicated after the initial PAAm deposition, but prior to nanodiamond deposition, using a Sonifier Cell Disruptor (Heat Systems Co., Model: W1850, Melville, NY). The particles were sonicated in 1 min intervals until they had been sonicated for a total of 5 min. Sonication was performed with the particles in the centrifuge tube that would later be used for deposition. Between sonications, the centrifuge tube was immersed in ice water for 1 min to prevent overheating of the sample. Other than this initial sonication, the particles were functionalized, cross-linked, and tested in the same manner as the previous batch of cross-linked particles. This resulted in particles with an improved particle size distribution (PSD) over the previous, nonsonicated batch.

Another batch of particles was prepared where sonication was performed after every PAAm deposition until the desired shell thickness was reached. Otherwise, these particles were prepared in the same manner as the previous batches. This approach yielded the tightest PSD of the three preparation methods.

Compared to the case of the uncoated particles, in all of the particle syntheses a significant increase in the mass and volume of the particles was observed after the LbL depositions.

Particle Functionalization. Core−shell particles made through deposition of 30 PAAm/nanodiamond bilayers, and terminated with a PAAm coating, were rinsed three times in 2-propanol and three times in 1:1 cyclohexanol:xylenes. The particles were then placed in ca. 15 g of the cyclohexanol:xylenes solution to which functionalizing agents were added. To prepare a non-cross-linked phase, 10 wt % of 1,2-epoxyoctadecane was added. This was reacted with the particles in a round-bottom flask, which was fitted with a water-cooled condenser and heated to 130 °C for 54 h. For the cross-linked phase both 10 wt % of 1,2-epoxyoctadecane and 0.5 wt % of 1,2,7,8-diepoxyoctane were added. The diepoxide served as the cross-linker. The reaction conditions were the same in the preparation of the cross-linked and the non-cross-linked particles.

The reaction mixtures were allowed to cool to room temperature. Excess functionalizing reagent was removed by rinsing and centrifuging three times with the cyclohexanol:xylenes solution, three times with 2-propanol, and three times with a 1% (v/v) aqueous solution of Triton X-100.

Particle Sieving. After particle functionalization, the particle size distribution was measured. In the nonsonicated material, there were ca. 100 μm agglomerates, so the particles, in an aqueous solution of Triton X-100 (1% v/v), which worked as a dispersant, were passed through a 40 μm sieve, which removed most of the larger agglomerates. Although improved, the particle size distribution was still far from uniform (see Figure 10A). After sieving, the particles were concentrated by centrifugation.

Column Packing. Packing was performed by suspending the particles in 12 mL of an aqueous solution of Triton X-100 (1% v/v). The Triton solution was also used as the pushing solution during packing. The slurry was poured into the packing chamber which had a 30 mm × 4.6 mm i.d. column attached at its end. The maximum packing pressure was set at 7000 psi (8500 psi for the improved (sonicated) particles). Packing occurred over a 25 min period and the pressure was released gradually over a 30 min period.

Another column (50 mm × 4.6 mm i.d.) was packed at the University of Tasmania using a pump from Haskel (Burbank, CA). The particles were suspended in 2-propanol and packed at 8000 psi until 25 mL of packing solvent had passed through the column. An insufficient volume of particles was used on the first attempt, so the column was repacked with a mixture of new and previously packed d_p = 4 μm particles. This second attempt was successful.

Stability Tests. Two stability tests were performed on the cross-linked material. The first was run under the following conditions: flow rate, 0.5 mL/min, mobile-phase composition, 40:60 H_2O:ACN with 0.1% (v/v) triethylamine in the aqueous portion of the mobile phase to set the pH at 11.3; temperature, 35.0 °C. The test occurred over 1600 column volumes. A stability test at pH 13.0 was then performed on this column. The mobile phase was 40:60 H_2O:ACN, with 1% (v/v) of the tetramethylammonium hydroxide solution (Table 1) in the aqueous component to raise the pH to 13. The column temperature was 35.0 °C. The test occurred over 1000 column volumes. The analytes used for these tests were from a benzenoid hydrocarbon kit and included benzene, ethylbenzene, *n*-butylbenzene, and *n*-hexylbenzene. After the stability tests, the HPLC system was flushed with ACN or MeOH and water for many minutes to remove the corrosive material that might damage the pump and/or detector flow cell. After use, the columns were also flushed with the same mobile phase and stored under MeOH between uses.

UHPLC and Sandwich Injection. A UHPLC system, Agilent Infinity 1290, with a diode array detector (Model No. G4212A, detection at 254 nm), an LC pump (Model No. G4220A), a column oven (Model No. G1316C), and an autosampler (Model No. G4226A), was used. This system was run with Chem Station Software, version B.04.03, and measurement of the fwhm by the software was used to calculate efficiencies. A "sandwich" injection on this system was performed using a mixture of alkylbenzenes. To wit, a 5 μL sample of an alkylbenzene analyte mixture was injected between 7 μL volumes of water onto our d_p = 4 μm column (see Figure 10c) at 80 °C using a pH 11.3 mobile phase, with a flow rate of 1.0 mL/min.

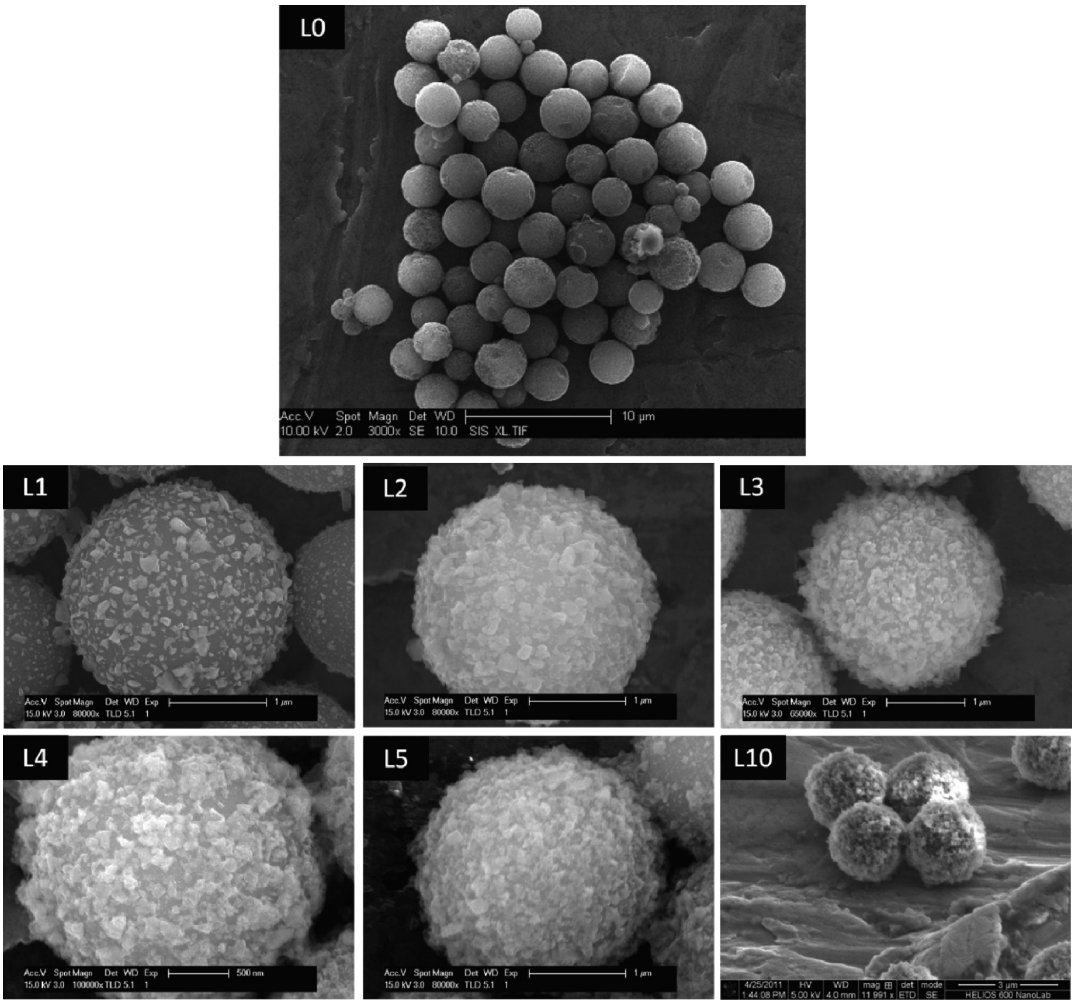

Figure 1. (L0) SEM image of the carbon core particles used in all the chromatographic studies of this document. (L1−L5, L10) SEM of LbL-coated model carbon particles, which were synthesized according to a procedure derived from the literature.[49−53] These particles were coated with nanodiamond that had a broad particle size distribution (ca. 10−400 nm, Advanced Abrasives). The particles were oxidized prior to the first PAAm deposition. Particles prepared with the nanodiamond with this broad PSD were not employed in any of the chromatographic studies described in this paper. It was advantageous to use these particles because they could be easily imaged by SEM. L1 refers to one bilayer of PAAm and nanodiamond, L2 refers to two bilayers of PAAm and nanodiamond, etc.

RESULTS AND DISCUSSION

Characterization of Core Particles and the LbL Process. The glassy carbon core particles, which are not commercially available and are a prototype material, were characterized by scanning electron microscopy (SEM), X-ray photoelectron spectroscopy (XPS), time-of-flight secondary ion mass spectrometry (ToF-SIMS), and Raman spectroscopy. SEM showed that the glassy carbon cores were largely spherical but had a fairly broad particle size distribution (Figure 1, (L0)).

XPS analyzes the upper ca. 10 nm of a material, and gives insight into the elemental composition of surfaces of materials. An XP survey scan (Figure 2) of the core carbon material showed two main peaks from carbon (C1s) and oxygen (O1s), carbon comprising 83% of the surface, and oxygen the remaining 17%. These atomic percentages were acquired through XPS narrow scans. The presence of oxygen should be important for adherence of PAAm to the core particles.

ToF-SIMS, a form of surface mass spectrometry, provides chemical information about the upper ca. 3 nm of a surface and is sensitive to all elements. Consistent with the XPS, negative ion ToF-SIMS of the core particles showed fairly intense O^- and

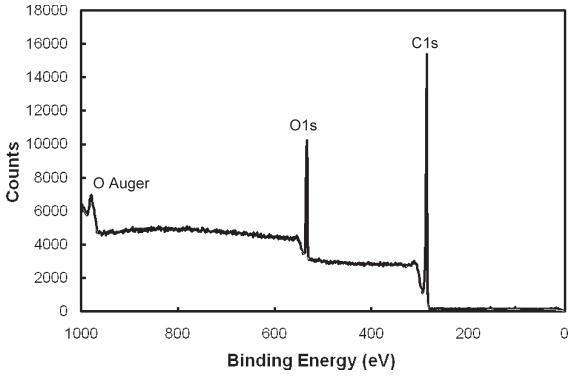

Figure 2. XPS of spherical carbon cores. The carbon (C1s) peak (286 eV) comprises ca. 83% of the surface while the oxygen (O1s) peak (534 eV) comprises the other ca. 17% of the surface.

dx.doi.org/10.1021/ac200436a |*Anal. Chem.* 2011, 83, 5488–5501

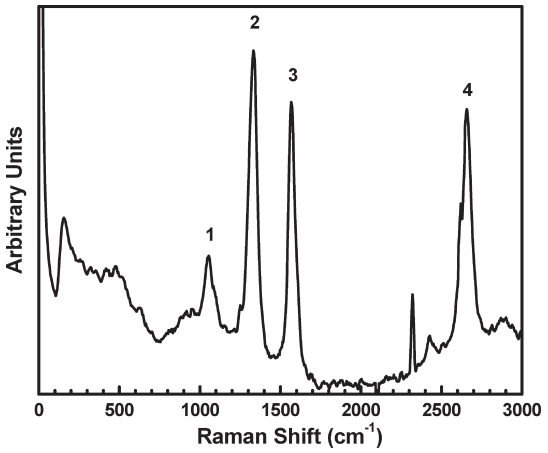

Figure 3. Raman spectrum acquired with 532 nm light. Band 1 is the T band (1050 cm^{-1}), corresponding to sp^3-bonded carbon. Band 2 is the D band, also corresponding to sp^3-bonded carbon (diamond-like). Band 3 is the G band, corresponding to graphitic, sp^2-bonded carbon. Band 4 is the G′ band, and is an overtone of the D band.

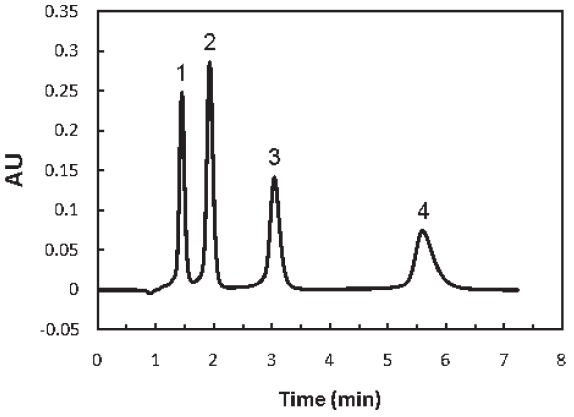

Figure 4. Reversed-phase separation of (1) benzene, (2) ethylbenzene, (3) *n*-butylbenzene, (4) *n*-hexylbenzene. Mobile phase: 40:60 H_2O:ACN with 0.1 (v/v)% triethylamine, pH 11.3. Flow rate 0.5 mL/min. Column temperature 35 °C. Detection at 254 nm.

OH^- peaks. It also showed the expected C^-, CH^-, C_2^-, and C_2H^- signals (Figure 1 in the Supporting Information).

Raman spectroscopy gives the analyst information about the degree of sp^3- or sp^2-bonding in a bulk carbonaceous material.[54,55] The Raman spectrum in Figure 3 contains four distinct peaks labeled 1−4. Peak 1 represents the T band. It is centered around 1050 cm^{-1} and can be assigned to sp^3-bonded carbon.[56] Peak 2 is designated as the disorder-induced band (or D band). It is centered at approximately 1350 cm^{-1} and is also due to sp^3-bonded carbon (diamond-like carbon).[55,57,58] Peak 3 is designated as the G band and is centered around 1580 cm^{-1}. It is attributed to sp^2-bonded carbon (graphitic type bonding).[55,58] Peak 4, which is centered around 2700 cm^{-1}, is the G′ band, which is an overtone of the D band.[57] It is clear from this spectrum that both sp^2- and sp^3-hybridized carbon are present in the particles.

To track the coating process on a spherical carbon material, we prepared core−shell particles with nanodiamond larger than those used for our packed pellicular phases. This made it easier to follow the LbL process by SEM (see Figure 1). It is clear from Figure 1 that the core material is nearly completely coated after five deposition cycles and that nanodiamond deposition progresses steadily from deposition to deposition. It should also be noted that, despite calling our deposition process "layer-by-layer," a complete layer is not obtained after each deposition, which is consistent with previous results.[48] Finally, note that the spherical carbon material used to obtain the SEM images in Figure 1, L1−L5, L10, is different from that employed for the packings used in the chromatographic studies in this paper. Nevertheless, this should be a representative study, as the LbL of PAAm and nanodiamond has now been shown to proceed on micrometer-sized diamond particles,[48] planar silicon surfaces,[48] and the other carbon cores used in this study.

Non-Cross-Linked, Hydrophobic Phase. The first batch of core−shell particles made from carbon cores and PAAm/nanodiamond shells was not cross-linked. In the formation of these (and subsequent) particles, the PAAm was expected to deposit as an ultrathin film in a self-limiting fashion.[42,48] The primary amines from the PAAm in the shell layer were only reacted with monofunctional 1,2-epoxyoctadecane resulting in a C_{18} phase. Chromatography was performed on this column using alkylbenzene analytes (see separation conditions in the caption to Figure 4). Under all conditions explored, peaks showed a large amount of fronting regardless of analyte concentration. This may be due to nonuniform column packing. Moreover, the non-cross-linked column showed a rapid increase in back pressure over a short period of time which indicated mechanical instability of this material.

During our experimentation with this column, the flow rate was doubled from 0.5 to 1.0 mL/min. Upon returning to the original flow rate, the back-pressure had increased significantly from 2040 to 3620 psi. After this experiment, the back-pressure steadily increased over a 6 h period to 4570 psi. At this point, the experiment was terminated. We had previously observed mechanical instability with non-cross-linked phases in our lab,[48] so we opted for a different approach that included cross-linking, with the hope that a more mechanically stable phase could be created.

Cross-Linked, Hydrophobic Phases. *Surface Area, Pore Size, and Volume.* The surface area of the cross-linked particles was 44.2 m^2/g by BET isotherm measurements. The particles had a mean pore size of 28 nm and a pore volume of 0.356 cm^3/g.

Pressure-Flow Relationship and Hydrophobic Character. To determine the effect of cross-linking, the column was reacted with 1,2-epoxyoctadecane under the same conditions as described above, but with the addition of a small amount of cross-linker: 1,2,7,8-diepoxyoctane. The resulting cross-linked stationary phase was then packed under the same conditions as the previous column. From the chromatography, it was immediately clear that this phase was less hydrophobic than the non-cross-linked phase, which would be consistent with the incorporation of the diepoxide into the stationary phase. That is, the diepoxide, which contains eight carbon atoms and will yield two hydroxyl groups upon reaction with PAAm, is less hydrophobic than 1,2-epoxyoctadecane, which contains eighteen carbon atoms and will only yield one −OH group when it reacts with PAAm. For example, under the same conditions used with the non-cross-linked column (mobile phase and pressure), the last eluting peak, *n*-hexylbenzene, eluted about 1.5 min earlier. Figure 4 shows the chromatogram of this and other alkylbenzenes on this cross-linked column. There were also immediate indications that this cross-linked material would be stable over a longer period of time, as evidenced by our ability to increase and decrease repeatedly and reproducibly the

mobile-phase velocity. A plot of the resulting linear relationship between pressure and flow is shown in Figure 5.

To compare the hydrophobicity of our materials to the hydrophobicity of other columns, we calculated log k for a series of alkylbenzenes: benzene, toluene, ethylbenzene, *n*-butylbenzene, and *n*-hexylbenzene,[59] and then fit the data to the equation

$$\log k = \alpha(CH_2)C_n + \beta(Ph) \quad (1)$$

where $\alpha(CH_2)$ and $\beta(Ph)$ are the retention increments for the methylene and phenyl groups respectively, and C_n is the number of carbon atoms in the side chain of the alkyl benzene.[59] That is, the interaction of the stationary phase with the phenyl group will give the *y*-intercept and that with the methylene units will provide the slope. The value of $\alpha(CH_2)$ thus gives an indication of the hydrophobicity of a column.

One of our columns (4 μm mean particle size, 30 mm × 4.6 mm i.d. column, see Figure 10c) that was used for many months prior to this test was evaluated and gave an $\alpha(CH_2)$ of 0.15 under 40:60 (0.1% TEA):ACN at 30 °C. Another column (4 μm mean particle size, 50 mm × 4.6 mm i.d. column, packed in Tasmania) was tested at the beginning of its lifetime and gave an $\alpha(CH_2)$ of 0.19 under 55:45 water:ACN at 60 °C. This difference in $\alpha(CH_2)$ values is attributed to different mobile-phase conditions, column ages, and operating temperatures. These data were compared to a previous study by Smith et al.[60] reported for a Spherisorb ODS-2 octadecyl-modified silica gel. From the retention factors of alkylbenzenes that were separated in a 20 mM sodium phosphate buffer (pH 7.0):ACN mobile phase (40:60 v/v) at 30 °C we calculate an $\alpha(CH_2)$ value of 0.17. This comparison points to a substantial hydrophobic (RP) character for our materials.

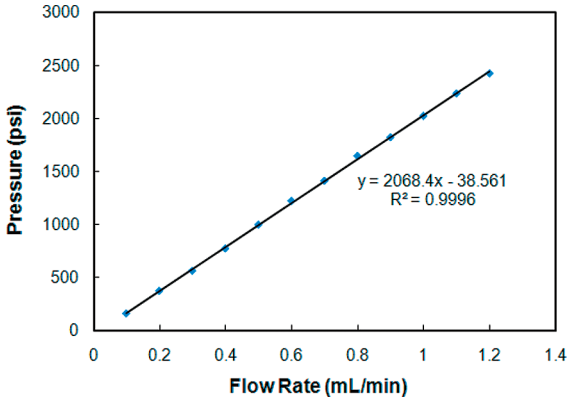

Figure 5. Pressure vs flow curve for the cross-linked column. Pressures obtained at different flow rates were reproducibly observed as the flow was varied.

As a further note of comparison, the initial back-pressure for the column containing the cross-linked phase was 940 psi, while the starting pressure for the column containing the non-cross-linked phase was 2040 psi. (Both columns were packed under identical conditions.) These results for the non-cross-linked particles suggest mechanical instability during packing, which would lead to clogging of the frit or the interstitial spaces between the particles by fines, possibly sloughed off the particles during column packing. However, even the back pressure from the column containing cross-linked material was higher than might be expected for a column containing 4 μm particles. To probe this issue, the back frit (closer to the detector) from one such column, which had been used extensively, was removed and analyzed by SEM. The resulting micrographs suggested plugging of the frit (Figure 2 of the Supporting Information). In the future, it will be determined whether the plugging came as a result of fines that were not removed prior to packing, or as a result of damage to the particles during packing. At present, the data point to the former explanation.

Stability at pH 11.3. The first stability test performed on the cross-linked column took place over 1600 column volumes of mobile phase at pH 11.3. The flow rate was 0.5 mL/min, and the column temperature was 35 °C. An analyte mixture containing benzene, ethylbenzene, *n*-butylbenzene, and *n*-hexylbenzene was used to probe the column during this test. The trial ran over a 26.6 h period and resulted in a decrease in k of 4.2−6.1% (see Figure 6). The efficiency (N/m) of the column decreased initially; however, it recovered and over the length of the test there was no overall decrease in its efficiency (see also Figure 6).

Stability at pH 13.0. A second stability test was then performed on this same column at pH 13.0 using the same analyte mixture (Figure 7). The mobile phase was 40:60 H_2O:ACN with the aqueous portion set at pH 13.0 by addition of 1% (v/v) tetramethylammonium hydroxide solution. The flow rate for

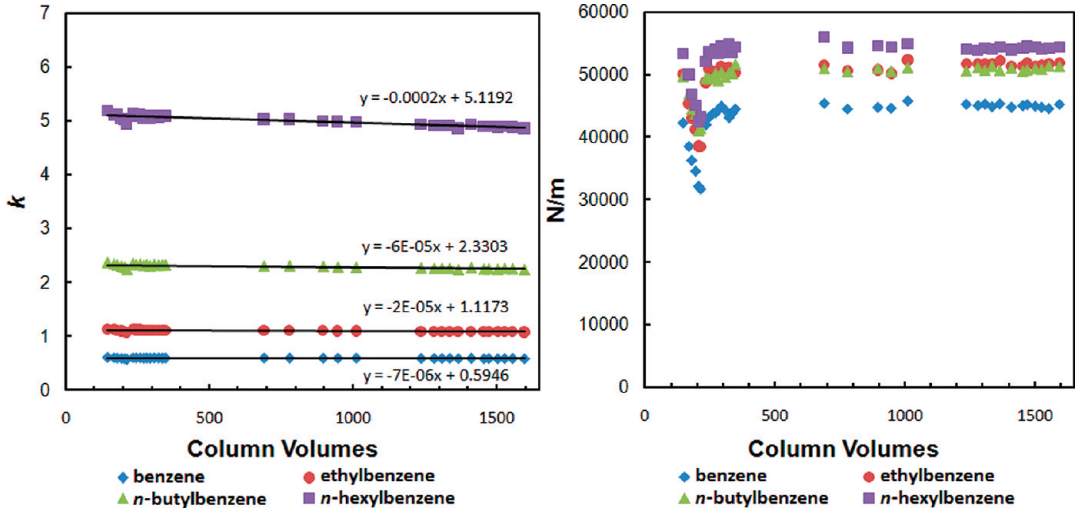

Figure 6. Column stability test at pH 11.3. See text for experimental details.

dx.doi.org/10.1021/ac200436a |*Anal. Chem.* 2011, 83, 5488–5501

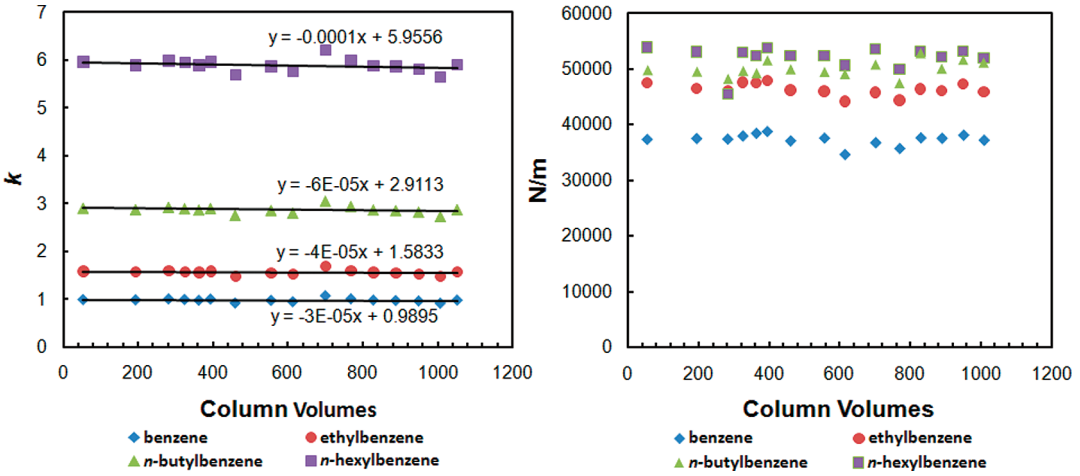

Figure 7. Stability test at pH 13.0 on the same column used for Figure 6. See text for experimental details.

Table 2. Van Deemter Terms and Optima for Each Analyte

	A (μm)	B (μm*mL/min)	C (μm*min/mL)	R^2	flow rate$_{opt}$ (mL/min)	H_{opt} (μm)
benzene	8.45	2.31	22.8	0.99955	0.32	23.0
ethylbenzene	6.36	2.62	18.8	0.99924	0.37	20.4
n-propylbenzene	5.71	2.74	17.4	0.99967	0.40	19.5
n-butylbenzene	3.89	3.25	16.8	0.99958	0.44	18.6

this stability test was 0.5 mL/min, and the column temperature was 35.0 °C. Over the course of this stability test, only a slight decrease (ca. 1%) in k was seen. Given the scatter in the data, it was not possible to conclude whether the efficiencies of the columns increased or decreased; they remained nearly constant. (After a careful scrutiny of the data, one might argue that a small decrease in efficiency of ca. 2−3% occurred for most of the analytes, although the efficiency for *n*-butylbenzene appeared to *increase* by ca. 3%.) Overall, we can state that little or no change took place in column properties and that this phase shows the greatest stability of any HPLC phase we have created to date.

Van Deemter Study and Instrument Response. The reasonable back-pressures of this column opened the possibility of varying flow rates enough to obtain van Deemter curves. For this study, the mobile phase was the same as that used for the first stability test (pH 11.3). An analyte mixture consisting of benzene, ethylbenzene, *n*-propylbenzene, and *n*-butylbenzene was used, and measurements were taken every 0.1 mL/min from 0.1 to 1.2 mL/min. Table 2 gives the results of this van Deemter study, and Figure 8 shows a representative van Deemter curve for *n*-butylbenzene, the best performing analyte in this study. The optimal plate height and flow rate for *n*-butylbenzene from the fitted van Deemter data were 18.6 μm (which equates to ca. 53 800 N/m) and 0.44 mL/min. The best efficiency for a single injection of *n*-butylbenzene was 56 000 N/m at 0.5 mL/min. A trend in this van Deemter study (Table 2) was that the A and C terms decreased as the analytes increased in molecular weight. Also shown in Table 2 is that with increasing analyte molecular weight, the optimal mobile-phase flow rate increased. Furthermore, the improvements we observed in efficiency with retention, which in our case also corresponds to analyte molecular weight, are consistent with extra column contributions to band broadening. The HPLC system used in this work had a dead

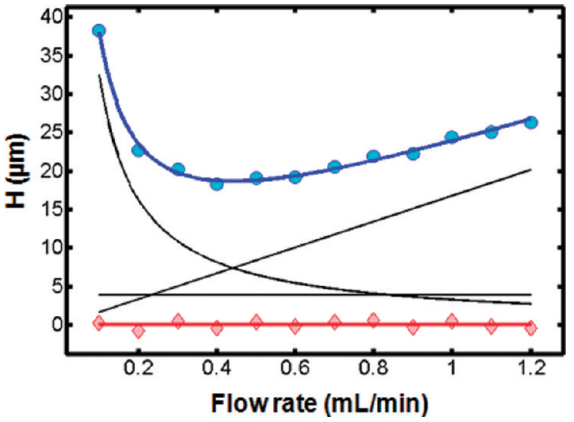

Figure 8. Van Deemter curve of *n*-butylbenzene. The raw data and residuals to the data are represented by the symbols: ○ and ◊, respectively. The black lines represent the fitted A, B, and C terms.

volume of ca. 100−105 μL, which was within the specifications for this instrument. However, for earlier eluting analytes on our short columns, the LC appeared to contribute to decreased efficiencies.

It is significant that the plate counts observed on this column are higher than those for phases previously created in our lab,[48] despite previous phases having smaller particle sizes. The peaks also appear to have good asymmetries, although some of them show some fronting. Symmetry factors, which appeared to be low, could not be calculated for the separations in the van Deemter study because the peaks were not fully baseline separated (Figure 3 of the Supporting Information).

A "sandwich" injection of an alkylbenzene analyte mixture was done on a UHPLC system with the pH 11.3 mobile phase used

for the stability test in Figure 6. The column used was the one corresponding to Figure 10C. This UHPLC system was expected to have substantially lower extra column band broadening contributions than the HPLC system used for our other separations. This separation, which was performed once, pointed to the potential efficiencies of our diamond-based phases when used under more optimized conditions. In the resulting chromatogram (Figure 9), benzene, ethylbenzene, *n*-butylbenzene, *n*-hexylbenzene, *n*-octylbenzene, and *n*-decylbenzene showed efficiencies of 117 000, 120 100, 111 400, 80 900, 52 100, and 21 400 N/m, respectively. Not only did this separation give us much better efficiencies than those obtained previously, but later eluting analytes had lower efficiencies, which is a reversal of the results obtained with our HPLC. Obviously the chromatograph can strongly influence separations.

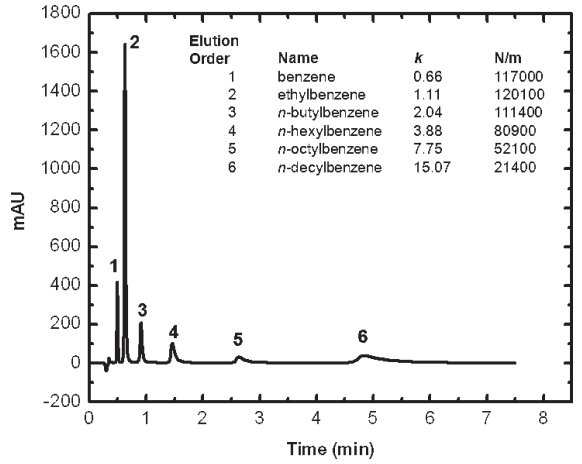

Figure 9. Separation obtained on an Agilent Infinity 1290 using a "sandwich" injection.

PSDs and SEMs of Particles and Particle Optimization. The reduced plate height, $h = H/d_p$, where d_p is the average particle diameter, of a well-packed column of good particles is typically 2. Accordingly, we were concerned with our higher than desired values of h (ca. 5 based on a projected particle size of 4 μm) and were also surprised that our *C* term had contributed so significantly to our overall plate height because we had created a phase based on a core−shell particle.

To obtain greater insight into these problems, we measured our particles' size distribution (PSD). Despite starting with a material with a 3 μm average particle size and a shell thickness of 0.5 μm (4 μm total), our measurements showed a mean particle size of 14.0 μm and a $D_{90/10}$ (skewness) of 3.9 after functionalization. This less-than-ideal PSD is shown in Figure 10A, which indicates a clear need for particle optimization. Scanning electron microscopy also suggested the presence of agglomerates in this material (Figure 4 of the Supporting Information).

Particle Optimization. Our next goal was to create a new batch of particles with the same cross-linked/C_{18} functionality, but with fewer agglomerates. In this effort, the particles were sonicated after the first PAAm coating (before LbL deposition). After particle formation, a substantially improved PSD was obtained (see Figure 10B), and the mean d_p of this batch was 5 μm. The column was characterized as before, and the resulting van Deemter curve showed the expected flattening of its *C* term. Whereas the *C* term for the previous particles was 16.8, the *C* term for the sonicated particles was 7.86. Unfortunately, the *A* term for this new column/material increased, which suggests that our packing procedure was not optimized. A third batch of particles was then created, where sonication was employed after every

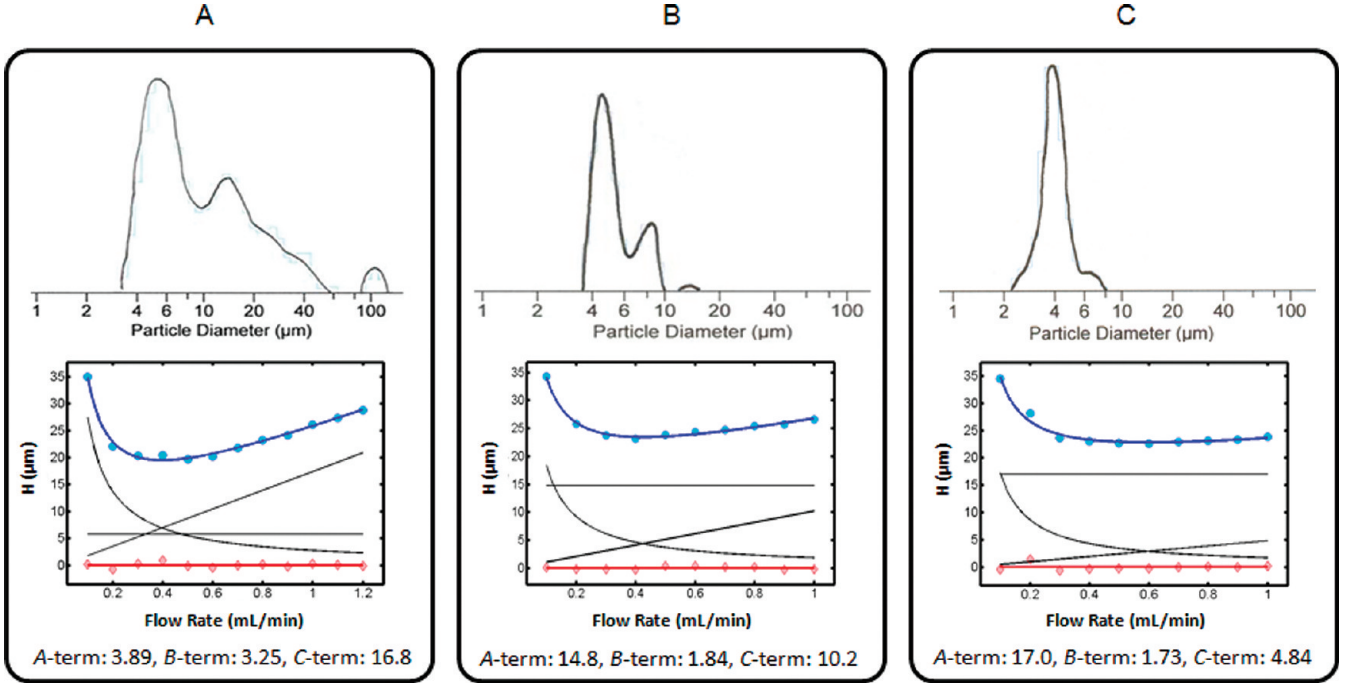

Figure 10. PSDs of core−shell particles synthesized in three different ways, and corresponding van Deemter curves from columns packed with these particles, with *n*-butylbenzene as analyte. For separation conditions see Figure 4. (A) Particles that were not sonicated prior to nanodiamond deposition. (B) Particles that were sonicated prior to the first nanodiamond deposition. (C) Particles that were sonicated prior to every nanodiamond deposition. The units on the *A*, *B*, and *C* terms are μm, μm·mL/min, and μm·min/mL, respectively.

dx.doi.org/10.1021/ac200436a |*Anal. Chem.* 2011, 83, 5488–5501

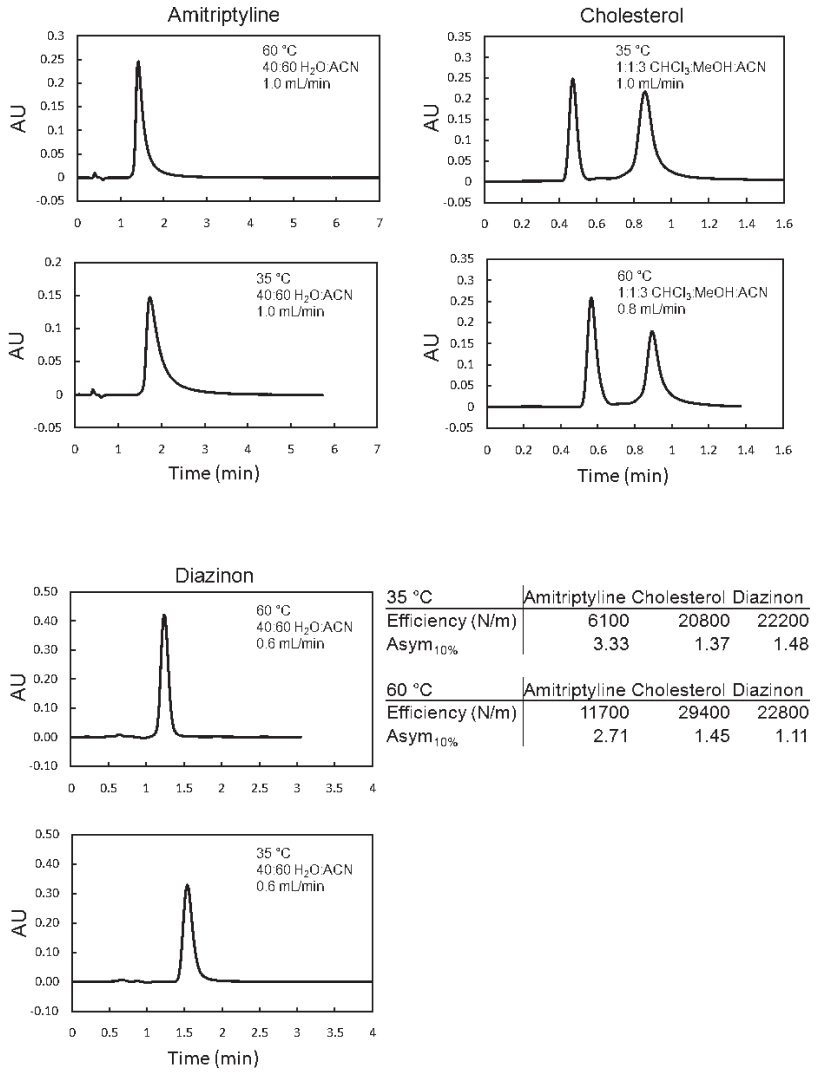

35 °C	Amitriptyline	Cholesterol	Diazinon
Efficiency (N/m)	6100	20800	22200
$Asym_{10\%}$	3.33	1.37	1.48

60 °C	Amitriptyline	Cholesterol	Diazinon
Efficiency (N/m)	11700	29400	22800
$Asym_{10\%}$	2.71	1.45	1.11

Figure 11. Effect of column temperature on the retention characteristics of amitriptyline, cholesterol, and diazinon using a high pH mobile phase (11.3).

PAAm deposition. This batch showed an even better PSD, with a mean d_p of 4 μm (see Figure 10C). The *C* term for these particles was even lower than before (4.84), but the *A* term remained high (17.0).

Retention and Separation of Various Analytes. *Retention of Amitriptyline, Cholesterol, and Diazinon at pH 11.3.* Diazinon (a pesticide), amitriptyline (a basic drug), and cholesterol (a lipid) were retained on our second column (d_p = 5 μm in Figure 10B). Better efficiencies and decreased asymmetries were seen at 60 °C, compared to 35 °C (Figure 11).

Retention of Amitriptyline and Three Organic Acids under Acidic Conditions. Under acidic conditions (40:60 0.1% formic acid:ACN) different retention mechanisms were seen for amitriptyline and various organic, aromatic acids. Amitriptyline was unretained at 35 and 60 °C. In this case it would be reasonable to assume that ion repulsion was occurring between amitriptyline and the stationary phase and this interaction overrode the hydrophobic character of the stationary phase.

Retention of toluic, benzoic, and *p*-chlorobenzoic acids was seen using a 100% methanol mobile phase containing 0.5 mM formic acid. Analytes exhibited substantial tailing. The trend in Table 3 is clear. Retention increases with decreasing pK_a (increased acidity) of analyte, consistent with an ion exchange interaction between the stationary phase and analytes.

Table 3. Retention of Various Benzoic Acids

acid	t_r (min)	$Asym_{10\%}$	pK_a
toluic acid	3.74	3.02	4.37
benzoic acid	4.90	2.73	4.20
p-chlorobenzoic acid	12.56	2.74	3.99

Separation of a Five-Component Pharmaceutical Mixture. A mixture of drugs, which included acetaminophen (Tylenol), diazepam (Valium), doxepin (Adapin), imipramine (Tofranil), and clomipramine (Anafranil), was separated at pH 11.3 using our third column (d_p = 4 μm) at 60 °C with a flow rate of 0.8 mL/min using a basic mobile phase of 40:60 water (0.1% TEA, pH 11.3):ACN (Figure 12). Some tailing was observed. We speculate that hydrogen bond acceptance and/or polar bonds of these basic analytes lead to interactions with the polar groups on the stationary phase, i.e., amine or hydroxyl groups. It is also possible that some of the nanodiamond surfaces may not be completely coated and any oxygenated

dx.doi.org/10.1021/ac200436a |*Anal. Chem.* 2011, 83, 5488–5501

moieties on those heterogeneous surfaces could also contribute to tailing of more polar analytes.

Separation of a Three-Component Pharmaceutical Mixture at pH 2.7. Separations at low pH were also attempted on the third column (Figure 10C, d_p = 4 μm), where the first group of analytes was acetaminophen, diazepam, and 2,6-diisopropylphenol (Propofol) (Figure 13A).

The mobile phase was 40:60 water (0.1% formic acid, pH 2.7):ACN. While acetaminophen and diazepam were retained longer than in the basic separation, their efficiencies were lower. We were pleased with the separation of Propofol from the analyte mixture. Propofol show higher efficiencies (48 300 N/m) than we had seen with the other non-alkylbenzene analytes, and the peak symmetry was very good. This led us to attempt a separation of various phenols at acidic pH.

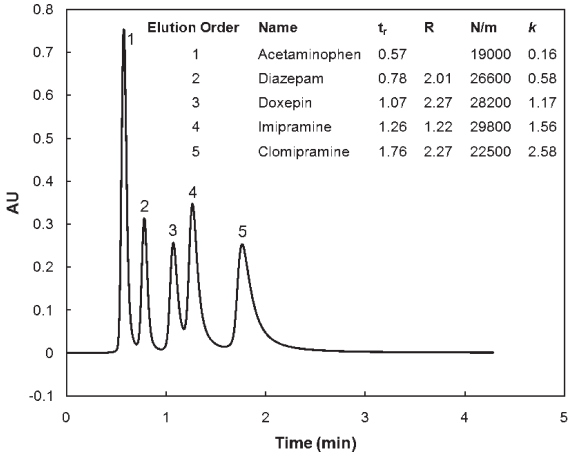

Figure 12. Separation of five pharmaceuticals. See text for separation conditions.

Separation of Phenolic Compounds and Derivatives at pH 2.7. Six phenolic compounds were separated using a mobile phase of 55:45 water (0.1% formic acid pH 2.7):ACN (see Figure 13C). All of these analytes separated with an efficiency of ca. 13 500 N/m or better. The less than optimal efficiencies could be attributed to the core−shell particles being packed into the column twice (see the Experimental Section). We were pleased to see fairly good resolution between the isomers 2-chlorophenol and 4-chlorophenol. A trend that seemed apparent from this separation was that electron withdrawing groups appear to cause greater tailing. This may be a result of an exposed diamond surface that retains the more deshielded aromatic ring. Peak asymmetries could not be determined for this separation because most of the compounds were not baseline separated.

Retention of Propofol. We again separated Propofol, and used a 70:30 water (0.1% formic acid, pH 2.7):ACN mobile phase. The greater retention for this compound can be explained by the increased water in the mobile phase, resulting in a plate count of 71 500 N/m and a peak asymmetry of 1.12.

Note that we see no signs of degradation of the column at low pH, which might be have been evidenced by an increase or significant decrease in its back-pressure, or by a noticeable loss of performance. It would appear that cross-linking of the PAAm prevents any substantial swelling of the material.

CONCLUSIONS

We have reported the formation of pellicular particles prepared from carbon cores and porous PAAm/nanodiamond shells for HPLC. The carbon cores, which are not commercially available,

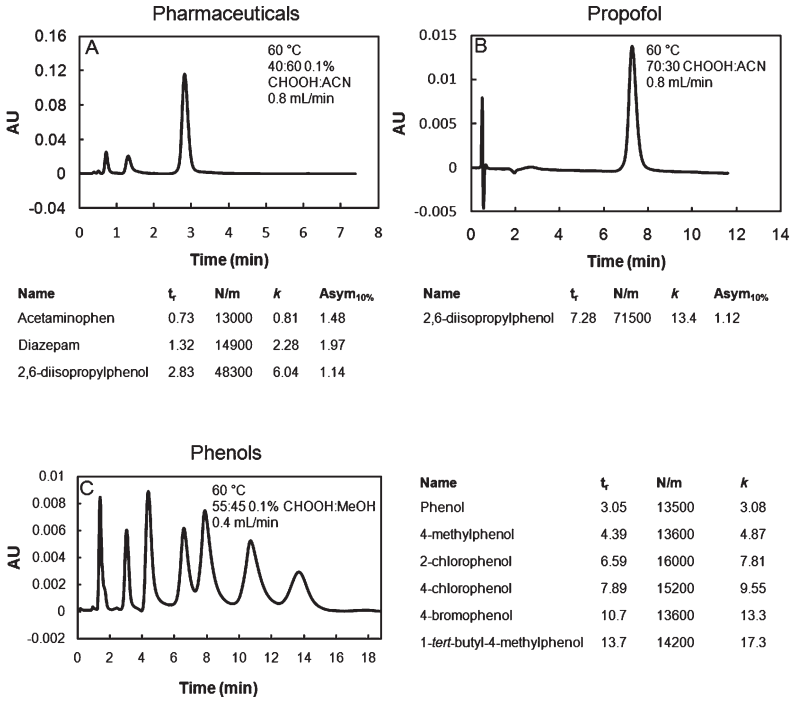

Figure 13. Separations of various analytes under acidic pH (2.7). Specific mobile-phase conditions are found next to the chromatograms. (A) Separation of three pharmaceuticals (acetaminophen, diazepam, and 2,6-diisopropylphenol) on the d_p = 4 μm column (Figure 10 C). (B) Retention of 2,6-diisopropylphenol (Propofol) on the same column. (C) A mixture of phenols (phenol, 4-methylphenol, 2-chlorophenol, 4-chlorophenol, 4-bromophenol, and 1-*tert*-butyl-4-methylphenol) separated using a 50 × 4.6 mm i.d. column.

dx.doi.org/10.1021/ac200436a |*Anal. Chem.* 2011, 83, 5488–5501

were characterized by XPS, ToF-SIMS, SEM, and Raman spectroscopy. We first developed a non-cross-linked C_{18} material. The resulting column appeared to be unstable, showed low efficiencies, and resulted in a significant increase in back-pressure over a short period of time, as had our previous non-cross-linked columns.[48]

Our next attempt to create a stable phase included the addition of a cross-linker (1,2,7,8-diepoxyoctane) during functionalization. The back pressures of this column were the lowest observed for any of our diamond-based core−shell particles to date. The pressure-flow behavior was completely reversible and allowed us to obtain a van Deemter curve for this phase. The optimal flow rate and theoretical plate height for our best performing alkylbenzene analyte, *n*-butylbenzene, were 0.44 mL/min and 18.6 μm, respectively. Our best results for a single injection of *n*-butylbenzene gave us 56 000 N/m. Unfortunately, our *A* and *C* terms were rather high.

Not only did the cross-linked phase show the best efficiencies yet seen for a diamond-based phase, ca. 71 000 N/m on a conventional HPLC, but it also exhibited good stability under extreme pH conditions: pH 11.3 and even pH 13. A "sandwich" injection on a UHPLC system showed best efficiencies of 110 000−120 000 N/m for three low molecular weight analytes.

Improvement in our particle size distributions was accomplished through sonication, which resulted in improved *C* terms for the columns packed with these particles. On the other hand, the *A* terms were higher. This was attributed to an unoptimized column packing procedure. Future work will focus on improving the column packing.

The columns packed with the sonicated phases were used to separate a more diverse set of analytes. Separations of pharmaceuticals at high (11.3) and low (2.7) pH were performed and phenols and phenolic derivatives were separated under acidic conditions. While no stability studies, per se, were performed under acidic conditions, there appeared to be no degradation of the phases under these conditions.

■ ASSOCIATED CONTENT

Supporting Information. (1) A MATLAB program, which conveniently plots van Deemter curves, including the individual contributions of the *A*, *B*, and *C* terms, the residuals to the fit, the values of *A*, *B*, and *C*, the rmse, and R^2 values for the fit, and the optimal values of *u* and H. (2) Additional data, including a ToF-SIMS spectrum of the unfunctionalized glassy carbon material from Supelco, SEMs of a frit from a packed column and an unused frit, a chromatogram representative of separations observed while obtaining our van Deemter curves, and an SEM image of the (agglomerated) core−shell particles that correspond to Figure 10A. This material is available free of charge via the Internet at http://pubs.acs.org.

■ AUTHOR INFORMATION

Corresponding Author

*E-mail: mrlinford@chem.byu.edu.

■ ACKNOWLEDGMENT

We thank Paul Ross from Supelco for providing us with the spherical glassy carbon particles that served as our core material, Michael Standing at BYU for operating the SEM, Grant Brown (BYU undergraduate) for help with sample and mobile-phase preparation, John Kimmel from Agilent for assistance with the UHPLC, US Synthetic for continued funding and support, and the ARC Discovery Grant of UTAS (DP110102046) for supporting the travel of M. Linford to Tasmania.

■ REFERENCES

(1) Miller, J. M. *Chromatography: Concepts and Contrasts*, 2nd ed.; John Wiley & Sons, Inc: Hoboken, NJ, 2005.
(2) Snyder, L. R.; Kirkland, J. J.; Glajch, J. L. *Practical HPLC Method Development*, 2nd ed.; John Wiley: New York, 1997.
(3) Kirkland, J. J. *J. Chromatogr., A* **2004**, *1060*, 9–21.
(4) Kirkland, J. J.; Glajch, J. L.; Farlee, R. D. *Anal. Chem.* **1989**, *61*, 2–11.
(5) Nawrocki, J. *J. Chromatogr., A* **1997**, *779*, 29–71.
(6) Wehrli, A.; Hildenbrand, J. C.; Keller, H. P.; Stampfli, R.; Frei, R. W. *J. Chromatogr., A* **1978**, *149*, 199–210.
(7) Roumeliotis, P.; Unger, K. K. *J. Chromatogr., A* **1978**, *149*, 211–224.
(8) Engelhardt, H.; Nikolov, M.; Arangio, M.; Scherer, M. *Chromatographia* **1998**, *48*, 183–189.
(9) Sagliano, N., Jr.; Floyd, T. R.; Hartwick, R. A.; Dibussolo, J. M.; Miller, N. T. *J. Chromatogr., A* **1988**, *443*, 155–172.
(10) Kirkland, J. J.; Adams, J. B.; van Straten, M. A.; Claessens, H. A. *Anal. Chem.* **1998**, *70*, 4344–4352.
(11) Kirkland, J. J.; van Straten, M. A.; Claessens, H. A. *J. Chromatogr., A* **1998**, *797*, 111–120.
(12) Kobayashi, A.; Takezawa, K.; Takasaki, H.; Kanda, T.; Kutsuna, H. *J. Chromatogr., A* **2005**, *1073*, 163–167.
(13) Trammell, B. C.; Ma, L.; Luo, H.; Jin, D.; Hillmyer, M. A.; Carr, P. W. *Anal. Chem.* **2002**, *74*, 4634–4639.
(14) Trammell, B. C.; Ma, L.; Luo, H.; Hillmyer, M. A.; Carr, P. W. *J. Chromatogr., A* **2004**, *1060*, 61–76.
(15) Cheng, Y. F.; Walter, T. H.; Lu, Z.; Iraneta, P.; Alden, B. A.; Gendreau, C.; Neue, U. D.; Grassi, J. M.; Carmody, J. L.; O'Gara, J. E.; Fisk, R. *LC-GC* **2000**, *11*, 1162.
(16) Wyndham, K. D.; Lawrence, N.; Glose, K.; Cook, J.; Walsh, D.; Brousmiche, D.; Iraneta, P.; Alden, B.; Boissel, C.; Walter, T. *Polym. Prepr. (Am. Chem. Soc., Div. Polym. Chem.)* **2007**, *48*, 278–279.
(17) Wyndham, K. D.; O'Gara, J. E.; Walter, T. H.; Glose, K. H.; Lawrence, N. L.; Alden, B. A.; Izzo, G. S.; Hudalla, C. J.; Iraneta, P. C. *Anal. Chem.* **2003**, *75*, 6781–6788.
(18) Teutenberg, T.; Hollebekkers, K.; Wiese, S.; Boergers, A. *J. Sep. Sci.* **2009**, *32*, 1262–1274.
(19) McCalley, D. V. *J. Chromatogr., A* **2010**, *1217*, 858–880.
(20) McCalley, D. V. *Advances in Chromatography*; CRC Press: Boca Raton, FL, 2008; Vol. 46.
(21) Gagliardi, L. G.; Castells, C. B.; Ràfols, C.; Rosés, M.; Bosch, E. *Anal. Chem.* **2006**, *78*, 5858–5867.
(22) Haky, J. E.; Vemulapalli, S.; Wieserman, L. F. *J. Chromatogr., A* **1990**, *505*, 307–318.
(23) Knox, J. H.; Kaur, R. P. *Advances in Chromatography*; CRC Press: Boca Raton, FL, 1997; Vol. 37.
(24) Nawrocki, J.; Rigney, M.; McCormick, A.; Carr, P. W. *J. Chromatogr., A* **1993**, *657*, 229–282.
(25) Tanaka, N.; Araki, M. *Advances in Chromatography*; CRC Press: Boca Raton, FL, 1989; Vol. 30.
(26) Trüdinger, U.; Müller, G.; Unger, K. K. *J. Chromatogr., A* **1990**, *535*, 111–125.
(27) Nawrocki, J.; Dunlap, C.; McCormick, A.; Carr, P. W. *J. Chromatogr., A* **2004**, *1028*, 1–30.
(28) Sun, L.; Carr, P. W. *Anal. Chem.* **1995**, *67*, 3717–3721.
(29) Sun, L.; McCormick, A. V.; Carr, P. W. *J. Chromatogr., A* **1994**, *658*, 465–473.
(30) Nawrocki, J.; Dunlap, C.; Li, J.; Zhao, J.; McNeff, C. V.; McCormick, A.; Carr, P. W. *J. Chromatogr., A* **2004**, *1028*, 31–62.

(31) Cazes, J. *Encyclopedia of Chromatography*, 1st ed.; Marcel Dekker: New York, 2004.
(32) Rigney, M. P.; Weber, T. P.; Carr, P. W. *J. Chromatogr., A* **1989**, *484*, 273–291.
(33) Blackwell, J.A. *Chromatographia* **1993**, *35*, 133–138.
(34) Blackwell, J. A.; Carr, P. W. *J. Chromatogr., A* **1991**, *549*, 59–75.
(35) Blackwell, J. A.; Carr, P. W. *J. Liq. Chromatogr. Relat. Technol.* **1991**, *14*, 2875–2889.
(36) Pereira, L. *J. Liq. Chromatogr. Relat. Technol.* **2008**, *31*, 1687–1731.
(37) West, C.; Elfakir, C.; Lafosse, M. *J. Chromatogr., A* **2010**, *1217*, 3201–3216.
(38) Nesterenko, P.N.; Haddad, P. *Anal. Bioanal. Chem.* **2010**, *396*, 205–211.
(39) Nesterenko, P. N.; Fedyanina, O. N.; Volgin, Y. V. *Analyst* **2007**, 403–405.
(40) Nesterenko, P. N.; Fedyanina, O. N.; Volgin, Y. V.; Jones, P. *J. Chromatogr., A* **2007**, *1155*, 2–7.
(41) Nesterenko, P. N.; Fedyanina, O. N. *J. Chromatogr., A* **2010**, *1217*, 498–505.
(42) Saini, G.; Gates, R.; Asplund, M. C.; Blair, S.; Attavar, S.; Linford, M. R. *Lab Chip* **2009**, *9*, 1789–1796.
(43) Saini, G.; Yang, L.; Lee, M. L.; Dadson, A.; Vail, M. A.; Linford, M. R. *Anal. Chem.* **2008**, *80*, 6253–6259.
(44) Saini, G.; Wiest, L. A.; Herbert, D.; Biggs, K. N.; Dadson, A.; Vail, M. A.; Linford, M. R. *J. Chromatogr., A* **2009**, *1216*, 3587–3593.
(45) Yang, L.; Lua, Y. Y.; Tan, M.; Scherman, O. A.; Grubbs, R. H.; Harb, J. N.; Davis, R. C.; Linford, M. R. *Chem. Mater.* **2007**, *19*, 1671–1678.
(46) Yang, L.; Vail, M. A.; Dadson, A.; Lee, M. L.; Asplund, M. C.; Linford, M. R. *Chem. Mater.* **2009**, *21*, 4359–4365.
(47) Kirkland, J. J.; Langlois, T. J.; DeStefano, J. J. *Am. Lab.* **2007**, *8*, 18–21.
(48) Saini, G.; Jensen, D. S.; Wiest, L. A.; Vail, M. A.; Dadson, A.; Lee, M. L.; Shutthanandan, V.; Linford, M. R. *Anal. Chem.* **2010**, *82*, 4448–4456.
(49) Ramanathan, T.; Fisher, F. T.; Ruoff, R. S.; Brinson, L. C. *Chem. Mater.* **2005**, *17*, 1290–1295.
(50) Jee, A.-Y.; Lee, M. *Curr. Appl. Phys.* **2009**, *9*, e144–e147.
(51) Li, K.; Stöver, H. D. H. *J. Polym. Sci., Part A: Polym. Chem.* **1993**, *31*, 3257–3263.
(52) Downey, J. S. McMaster University, 2000.
(53) Li, L.; Song, H.; Chen, X. *Mater. Lett.* **2008**, *62*, 179–182.
(54) Jawhari, T.; Roid, A.; Casado, J. *Carbon* **1995**, *33*, 1561–1565.
(55) Ferrari, A. C.; Robertson, J. *Phys. Rev. B: Condens. Matter Mater. Phys.* **2000**, *61*, 14095.
(56) Silva, S. R. P. *Properties of Amorphous Carbon*. IEE: London, U.K., 2003; Vol. 29.
(57) Matthews, M. J.; Pimenta, M. A.; Dresselhaus, G.; Dresselhaus, M. S.; Endo, M. *Phys. Rev. B: Condens. Matter Mater. Phys.* **1999**, *59*, R6585.
(58) Nistor, L. C.; Van Landuyt, J.; Ralchenko, V. G.; Obraztsova, E. D.; Smolin, A. A. *Diamond Relat. Mater.* **1997**, *6*, 159–168.
(59) Penner, N.; Nesterenko, P.; Ilyin, M.; Tsyurupa, M.; Davankov, V. *Chromatographia* **1999**, *50*, 611–620.
(60) Smith, R. M.; Burr, C. M. *J. Chromatogr., A* **1989**, *475*, 57–74.